AD-A107 876 PENNSYLVANIA STATE UNIV UNIVERSITY PARK APPLIED RESE--ETC F/G 20/1
THE REVERBERATION AND ABSORPTION CHARACTERISTICS OF A WATER-FIL--ETC(U)
JUL 81 K A HOOVER N00024-79-C-6043
UNCLASSIFIED ARL/PSU/TM-81-150 NL

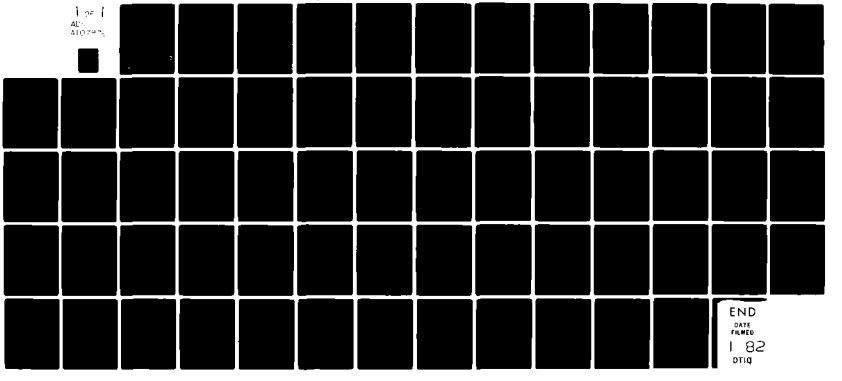

AD A107876

THE REVERBERATION AND ABSORPTION CHARACTERISTICS OF A WATER-FILLED CHAMBER WITH AND WITHOUT A PRESSURE-RELEASE WALL LINING

K. Anthony Hoover

Technical Memorandum
File No. TM 81-150
July 2, 1981
Contract No. N00024-79-C-6043

Copy No. 7

The Pennsylvania State University
Intercollege Research Programs and Facilities
APPLIED RESEARCH LABORATORY
Post Office Box 30
State College, PA 16801

DTIC FILE COPY

APPROVED FOR PUBLIC RELEASE
DISTRIBUTION UNLIMITED

DTIC ELECTE NOV 27 1981 D

A

NAVY DEPARTMENT

NAVAL SEA SYSTEMS COMMAND

105

SECURITY CLASSIFICATION OF THIS PAGE *(When Data Entered)*

REPORT DOCUMENTATION PAGE

READ INSTRUCTIONS BEFORE COMPLETING FORM

1. REPORT NUMBER: TM 81-150	2. GOVT ACCESSION NO.: AD-A114876
3. RECIPIENT'S CATALOG NUMBER:	
4. TITLE *(and Subtitle)*: The Reverberation and Absorption Characteristics of a Water-Filled Chamber With and Without a Pressure-Release Wall Lining	5. TYPE OF REPORT & PERIOD COVERED: MS Thesis, November 1981
	6. PERFORMING ORG. REPORT NUMBER: TM 81-150
7. AUTHOR(s): K. Anthony Hoover	8. CONTRACT OR GRANT NUMBER(s): N00024-79-C-6043
9. PERFORMING ORGANIZATION NAME AND ADDRESS: The Pennsylvania State University, Applied Research Laboratory, P.O. Box 30	10. PROGRAM ELEMENT, PROJECT, TASK AREA & WORK UNIT NUMBERS:
11. CONTROLLING OFFICE NAME AND ADDRESS: Naval Sea Systems Command, Department of the Navy, Washington, DC 20362	12. REPORT DATE: July 2, 1981
	13. NUMBER OF PAGES: 56 pages & figures
14. MONITORING AGENCY NAME & ADDRESS *(if different from Controlling Office)*:	15. SECURITY CLASS. *(of this report)*: Unclassified, Unlimited
	15a. DECLASSIFICATION/DOWNGRADING SCHEDULE:

16. DISTRIBUTION STATEMENT *(of this Report)*

Approved for public release, distribution unlimited, per NSSC (Naval Sea Systems Command), 8/21/81

17. DISTRIBUTION STATEMENT *(of the abstract entered in Block 20, if different from Report)*

18. SUPPLEMENTARY NOTES

19. KEY WORDS *(Continue on reverse side if necessary and identify by block number)*

acousitcs, underwater sound, reverberation, absorption, chamber

20. ABSTRACT *(Continue on reverse side if necessary and identify by block number)*

The requirements for a reverberation chamber in air have been described in the appropriate standards, but there is no mention that these same requirements cannot be applied to underwater reverberation chambers. A number of acoustic measurements were made to determine the reverberation time and absorption characteristics of an underwater chamber with and without a pressure-release wall covering. The reverberation times were found to be faster than the transient response times of conventional analog equipment. Therefore, a digital computer was employed to filter the data and to determine the slope,

DD FORM 1 JAN 73 1473 EDITION OF 1 NOV 65 IS OBSOLETE
S/N 0102-LF-014-6601

UNCLASSIFIED

SECURITY CLASSIFICATION OF THIS PAGE *(When Data Entered)*

and thus, the reverberation time by using a linear, least-squares curve fit. The pressure-release wall covering was found to reduce the average sound absorption coefficients to values acceptable for a reverberation chamber based on the standards for air acoustics.

ABSTRACT

The requirements for a reverberation chamber in air have been described in the appropriate standards, but there is no mention that these same requirements cannot be applied to underwater reverberation chambers. A number of acoustic measurements were made to determine the reverberation time and absorption characteristics of an underwater chamber with and without a pressure-release wall covering. The reverberation times were found to be faster than the transient response times of conventional analog equipment. Therefore, a digital computer was employed to filter the data and to determine the slope, and thus, the reverberation time by using a linear, least-squares curve fit. The pressure-release wall covering was found to reduce the average sound absorption coefficients to values acceptable for a reverberation chamber based on the standards for air acoustics.

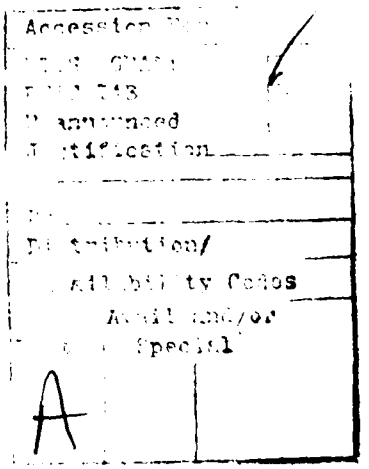

TABLE OF CONTENTS

LIST OF TABLES

LIST OF FIGURES

LIST OF FIGURES (continued)

ACKNOWLEDGEMENTS

The author wishes to thank Dr. Edward C. Andrews for giving this thesis direction, Mr. John J. Portelli and Mr. Edward V. Welser for help with digitizing and programming, and especially Dr. Robert W. Farwell for his constant guidance and encouragement.

This research was supported by the Applied Research Laboratory of The Pennsylvania State University under contract with the Naval Sea Systems Command.

CHAPTER I

BACKGROUND AND INTRODUCTION

1.1 Background

The sound power radiated by a mechanical system is one of the most important acoustical quantities which can be measured. Much information about the effect of system modifications on the noise radiated by the system can be determined by knowing the sound power. But in order to make accurate measurements of the sound power, it is essential to have some knowledge about the environment in which the system is operating. If the sound power output of a mechanical system and information about the environment are known, then other acoustical quantities can be predicted.

There are several methods by which to measure the sound power output of a mechanism. Each of these methods is intended to determine different aspects of the radiated sound, and has its own advantages and disadvantages. For example, in order to determine the directivity pattern of the radiated sound, free-field conditions such as in anechoic chambers are required. But directivity patterns are not needed in many cases, and the methods that produce them are long and difficult. Simpler methods using reverberation chambers can often be used instead.

There are two methods of determining the sound power output of a mechanism in a reverberant chamber; these are the direct and comparison methods, which are described in detail in American National

Standard (ANS) S1.21-1972.[1] The comparison method compares the sound pressure level in the reverberant field of a mechanism to the sound pressure level of a reference source of known sound power. The direct method determines the sound power output by measuring the sound pressure level in the reverberant field in a chamber for which the amount of absorption is known. The absorption is determined from measurements of the reverberation time and the total surface area and volume of the room. The procedure for measuring the reverberation time is described in ANS S1.7-1970 (ASTM C 423-66)(R1972).[2] Reverberation time is defined as the amount of time it takes for the sound pressure in an enclosure to decay by 60 decibels (dB) below its original value after the sound source has been turned off. The response of a receiver during the decay of the sound field is recorded, and the reverberation time is obtained by determining the slope of the decay. If a full 60-dB decay is not obtained, then the reverberation time is found by linear extrapolation of the slope of the recorded decay.

These methods are routinely used for determining the sound power output of mechanisms operated in air. At the present time, there are no standards which deal with water as the medium of propagation, but the standards for air acoustics do not specifically disallow using the same methods for water acoustics. In fact, the nature of the equations and requirements is such that any medium could be investigated if the correct parameters such as speed of propagation are used. However, there are some important differences between water and air which affect the degree to which the standards for air reverberation chambers can be adhered to for underwater reverberation chambers.

The major differences between water and air are the speed of sound propagation and the characteristic impedances. The speed of sound in water is approximately five times greater than in air. This means that wavelengths of given frequencies are also five times greater in water than in air, and in turn, a chamber in water acoustically appears to be five times smaller than a chamber of equal dimension in air. Therefore, the requirement that hydrophones and microphones be a minimum of one-half wavelength away from chamber surfaces and from each other is more difficult to achieve in water than in air. Characteristic impedance is also an important consideration because the impedance of water is so much greater than that of air. Most materials used for construction have characteristic impedances which come close to matching the impedance of water. Thus, the absorption of sound for most materials is greater in water than in air; furthermore, an air-water surface reflects sound better than the surface between water and a material such as concrete. As a result, a chamber of given size and construction is generally more reverberant in air than in water.

1.2 Introduction

The Machine Quieting Laboratory (MQL) located in the Applied Research Laboratory of The Pennsylvania State University is a facility devoted to measuring noise output of underwater machinery. Noise reduction programs in the MQL rely on a method of comparing the measured sound pressure level output of machinery before and after modifications, producing an indication of the relative effectiveness

of attempted noise reduction. The validity of these results depends on the assumption that the test environment has not changed in any way during the course of the measurements. Furthermore, this method is so dependent on the laboratory conditions that it is not possible to determine with any certainty what the sound radiated under field conditions will be. It is desirable therefore to use a method which directly measures the actual sound power output of the machinery in order to obtain an absolute value.

The sound power output of a mechanism can be measured by different methods; these methods usually depend on either an anechoic or a reverberant environment. Thus, the nature of the available facilities usually determines which method will be used. The MQL tank is neither anechoic nor reverberant, but is somewhere in between. If the average absorption coefficients could be lowered to an acceptable level, then methods requiring reverberant chambers could be adopted.

In order to determine whether the comparison method or the direct method should be used, several factors must be considered. Both methods assume that the source being tested is small. This assumption is precarious when applied to the MQL because the machinery being tested will usually occupy a substantial portion of the volume of the tank. The comparison method, in particular, has problems because of the difficulty in determining a suitable position for the reference source when it replaces the test machinery. Furthermore, the test machinery might not act as a small source, but rather as a more extended source. Thus, the comparison method by its very nature introduces too much uncertainty into the results. The direct method

cannot strictly adhere to the standard because of the relatively large size of the test machinery, but it does avoid the problems associated with the reference source altogether. For this reason, the direct method is more preferable than the comparison method.

The direct method requires the determination of the average sound pressure level in the reverberant field and the absorption present in the test chamber. The average sound pressure level in the MQL tank can be determined from the measuring system of the comparative noise reduction programs. However, the absorption characteristics of the MQL tank are not well known. The absorption coefficients must be determined from reverberation time measurements.

Measurements of the reverberation in the MQL tank were performed by Pallett and by Ricker. Their unpublished measurements were done for several widely-spaced frequency bands and their results are not detailed enough for use in sound power measurements, but they did indicate that the absorption in the tank was too high for a good reverberation chamber. Pallett suggested that the absorption might be lowered by covering the walls of the MQL tank with a pressure-release material. Fridrich began the study of the effect of a pressure-release material upon the average absorption in the test chamber, as is described in his master's thesis.[3] Fridrich designed and built the pressure-release wall covering using closed-cell Neoprene rubber, made extensive recordings of the decaying reverberation over a wide range of frequencies with and without the wall covering, and developed a digital computer program to filter the data and to plot the decay in order to arrive at a reverberation time.

1.3 Thesis Objective

The primary objective of this thesis is to determine the absorption characteristics of the MQL tank with and without the pressure-release wall covering. This is determined from reverberation time measurements employing the digital computer program developed by Fridrich.[3] Absorption coefficients are calculated from these reverberation times using both the Sabine and the Norris-Eyring reverberation equations; due to the inherent differences between the two equations, some differences in the resultant absorption coefficients are encountered. Furthermore, the effect of the presence of a metal cylindrical shell in the MQL tank on the reverberation times is investigated.

CHAPTER II

APPARATUS AND METHODS

2.1 The Machine Quieting Laboratory Tank and Apparatus

The MQL tank, wall covering, instrumentation, test conditions, and data-taking procedure are described in detail by Fridrich.[3] The MQL tank, as shown in Figures 1 and 2, is a rectangular tank, the walls of which are constructed of 0.3048-meter-thick concrete. The tank measures 7.62 meters by 2.44 meters by 2.44 meters, and when the tank is filled to a depth of 2.13 meters, the water-filled volume is 39.6 cubic meters. The total surface area of this volume of water is 80.0 square meters; 23.2% of this area is the water-air boundary at the top of the tank and the remaining 76.8% is the water-concrete boundary at the floor and walls of the tank.

The pressure-release wall covering is Rubatex G-231-N, which is a closed-cell neoprene rubber. Sheets of this material are 6.35 millimeters thick. For the test conditions which required the pressure-release wall covering, a single layer of this material was attached to the four walls, covering approximately 53.6% of the total surface area. The sound source used to excite the tank is a Massa projector fed random noise from a General Radio generator, first filtered into one-third-octave bands using a General Radio sound and vibration analyzer, then amplified by a CML power amplifier. The output of the CML amplifier was monitored using a Tektronix

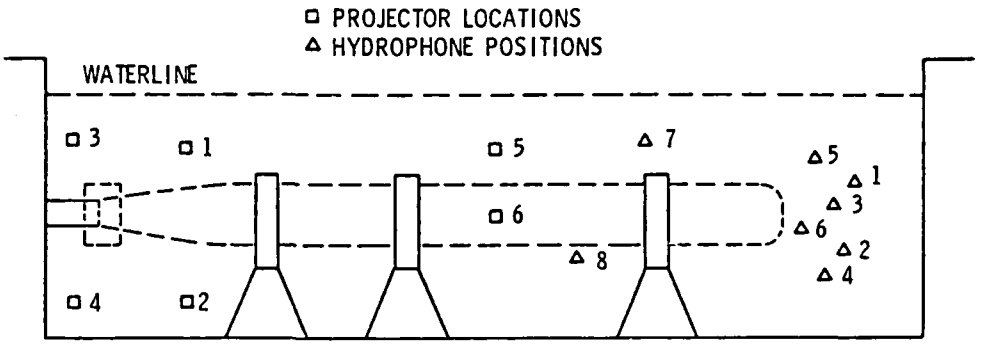

Figure 1. MQL Tank - Side view showing projector locations and hydrophone positions.

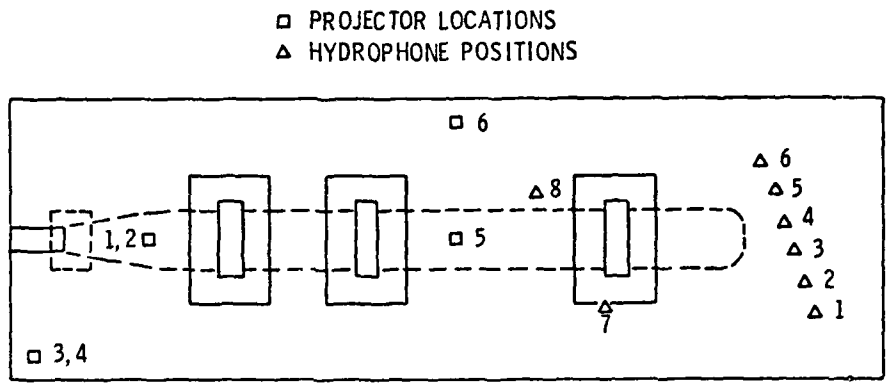

Figure 2. MQL Tank - Top view showing projector locations and hydrophone positions.

oscilloscope and a Brüel & Kjaer sound level meter. A toggle switch located between the one-third-octave filter and the power amplifier was used to turn off the projector; however, the response time of the amplifier was not investigated.

2.2 Projector Locations and Hydrophones

Six projector locations were used as shown in Figures 1 and 2. Projector locations one and two approximate the location of noise generating machinery that the MQL tank was designed to test. Projector locations three and four are located in the corners of the tank in order to excite the oblique modes as strongly as possible. Projector locations five and six are near the center of the tank.

Eight Bendix hydrophones were used to monitor the sound field; the signals from these hydrophones were recorded on 2/54-centimeter-wide Ampex magnetic tape using a fourteen-channel Sangamo tape recorder operated at a speed of 38 centimeters per second. The hydrophones were located at eight fixed positions as shown in Figures 3 and 4. Hydrophones 1 through 6 were located in positions used in previous noise reduction programs; hydrophones 7 and 8 were positioned arbitrarily, but purposely avoided close proximity to any major surface area of the tank, to the other hydrophones, or to regions which might be occupied by test machinery in the future.

2.3 Test Conditions

The reverberation time measurements were made under four test conditions. The differences between the test conditions are due to the presence or absence of the pressure-release wall covering, and

the presence or absence of a metal, cylindrical shell which was nearly as long as the tank. This shell was representative of a piece of machinery being tested in the MQL tank. Test condition I was bare tank and no shell; test condition II was bare tank with a shell; test condition III was tank lined with the pressure-release wall covering but no shell; and test condition IV was lined tank with a shell. For each test condition, the projector was moved to each of six positions. The center frequency of the one-third-octave-band filter was varied at each projector location so as to cover a range from 1 kHz to 16 kHz for a total of thirteen center-band frequencies. For each center-band frequency, the decay was recorded twice, resulting in two data sets. Using eight hydrophones, 1248 decays were recorded for each test condition. Thus, the total number of decays recorded for the four test conditions was 4992.

2.4 Initial Considerations

In order to determine reverberation time, the recorded signal of the decaying sound field is filtered to the desired one-third-octave band and the logarithm of the output is plotted as signal level versus time. The reverberation time is the time interval in which the signal level drops 60 dB; since it is rate that a full 60-dB range occurs, the extrapolation of the linear portion of the decay is used. The reverberation time of a chamber filled with water is much shorter than that of a chamber filled with air. Equipment normally used for reverberation measurements in air cannot be used; extremely fast response times are needed.

Fridrich[3] investigated three types of analysis methods: an analog analysis method, a hybrid analysis method, and a digital analysis method. In the analog analysis method, the chart recorder and the filter each responded too slowly to reveal the reverberation time. The hybrid analysis method inserted a transient store device into the analog system which allows for slower paper and pen speeds in the chart recorder, but the response time of the filter itself was still too close to the reverberation times of the recorded data. Thus, another method of filtering the data was sought. A digital analysis method was chosen by which the desired filtering characteristics were approximated using Fast Fourier Transforms. This procedure necessitated the digitization of the data originally recorded on tape in analog form, and the development of a digital computer program by which the filtering could be accomplished.

2.5 Digital Analysis Method

This filtering procedure divides the digitized data into consecutive time blocks, then an FFT is performed on each block in the time domain to produce a block of data in the frequency domain. The output of the FFT's corresponds to the power in consecutive segments of the frequency spectrum. Filtering is accomplished by considering only those segments of the frequency spectrum which correspond to the desired one-third-octave bands and ignoring the rest.

Since digital techniques are being used, a linear, least-squares curve fit can also be performed to determine the slope of the decay. This method of determining the slope, and in turn, the reverberation time, is more consistent than can be done in analog form. The reason

for this is that instead of trying to choose the best fit to the slope of the decay, all that need be done is choose the data over which the fit is to be performed, or in other words, choose the points at which the excitation signal ends and where the background noise becomes the predominant signal.

Digital techniques require that the analog data be converted into a digital form. Through the course of the project, two digitizing systems were used. The major differences between the original and final systems were the method by which the portion of data to be digitized was identified, the reliability of the components in the system, and the amount of time in which the digitizing could be accomplished.

2.5.1 Original digitizing system. For the original system,[3] preliminary analysis of the spectra of recorded data showed analog signals up to 25 kilohertz (kHz). The sample rate necessary for digitization is twice the highest frequency, or in this case, 50 kHz. A sample rate of 51200 samples per second was chosen because a power of two is convenient in this work. But 51200 samples per second was faster than any available equipment could handle, so the analog tape was played at a speed reduction of 4 to 1 while the digitizer operated at 12800 samples per second. Also, the low-pass anti-aliasing filter was set at 6 kHz, corresponding to an effective cut-off frequency of 24 kHz in real time. In addition to the speed reduction, the tape was played back in reverse. This was done for two reasons; first, the envelope detector which was used to locate the decay of the sound field would be most effective by sensing a build-up of signal level,

and second, the digital computer program which would actually determine the reverberation times would also make use of this build-up as it searched through the digital data to locate the decay.

After passing through the anti-aliasing filter, the signal was split to follow two paths. The first path primarily located the decay, and it consisted of an envelope detector, a voltage comparator, a flip-flop, a one-shot, and the A/D, or analog-to-digital, control. The envelope detector produced a voltage which was proportional to the magnitude of the waveform, and the voltage comparator compared the output of the envelope detector to a reference voltage which corresponded to the magnitude of the background noise. In this way, when the voltage produced by the envelope detector became equal to or greater than the reference voltage, the decay had been located. At this point, the flip-flop activated the one-shot which prescribed the amount of time for which the digitizer was to be operating on the data signal. The second path fed the signal into another tape drive which served as an analog delay. Since the record and playback heads were separated by 8.89 centimeters and the tape was played at 9.5 centimeters per second, the resultant delay was about 933 milliseconds. In effect, this delay allowed the digitizer to be activated slightly before the decay occurred. Since it was the delayed signal which was actually digitized, the delay allowed some of the background noise to be digitized.

The end result was a window of digitized data which represented a reverse image of the decay of the sound field in the MQL tank, complete with a portion of the background noise and the excitation signal. This digitized window of data was recorded on a digital tape

drive. Each window, or data point, was encoded with an identification number and a file mark was recorded after each window, so that each decay was uniquely identified.

Unfortunately, this system had many problems with the reliability of available equipment. To monitor the reliability of the system, a computer program called DCHECK was written. DCHECK located a particular identification number and file mark on the digital tape and determined whether any data had been recorded. DCHECK was routinely and necessarily run on every third or fourth data point.

Another problem with the digitizing system was the inordinate amount of time required to do the digitizing. Only one data point could be digitized at a time. Also, there was on average a two-minute time period between decays on the analog tape, and with a four-to-one tape-speed reduction, there could be an eight-minute wait between digitizing attempts. Even with fast-forwarding the tape, only a portion of the eight-minute wait could be eliminated without risking fast-forwarding beyond the decay itself. In spite of constant repair and piece-meal updating, this method of digitizing was eventually deemed unacceptable.

2.5.2 Final digitizing system. In order to improve the process, a completely different digitizing system was developed. Much of the problem with the first system was due to the method and equipment by which the decay was located. The new system employed a much simpler, manual approach. A time code was recorded directly onto the analog data tapes on an unused track. Each tape was then strip-charted, showing the position of the decays in relation to the time

codes. The time codes corresponding the position of the decays were specified. Then, four-second windows containing the decays were digitized, including approximately two seconds before the decay and two seconds after the decay.

Figure 3 is a block diagram of the strip-charting process. A one-pulse-per-second signal, produced by a Datum, Inc. time code reader (Model 9310), was recorded using a Honeywell tape recorder/ playback unit (Model 9600) onto channel 11 of the analog data tapes, which had been a blank channel. Two of the data channels, channels 1 and 2, were then passed through Spectrum, Inc. low pass filters (Model LH-42D) set at 6 kHz with a roll-off of 24 dB per octave. Each channel was then passed through an envelope detector, designed and built at the Applied Research Laboratory located at The Pennsylvania University, so that the strip-chart recorder would respond to the envelope of the signal. Both envelope detectors were set to a bandwidth of 100 hertz (Hz), allowing the strip-chart recorder to respond at 100 Hz instead of requiring up to 6000 Hz and still reveal the position of the decay relative to the time code. A Gould 6-channel strip-chart recorder (Model MK260), operated at a chart speed of 1 millimeter per second, recorded the data channels and the time code side by side so that the time code corresponding to the decay could be easily located; data channels 1 and 2 were recorded on strip-chart channels 4 and 5, and the time code channel was recorded on strip-chart channel 6.

As the time code corresponding to each decay was identified, the time codes corresponding to two seconds after and two seconds before the decay were noted so that a four-second window of data to

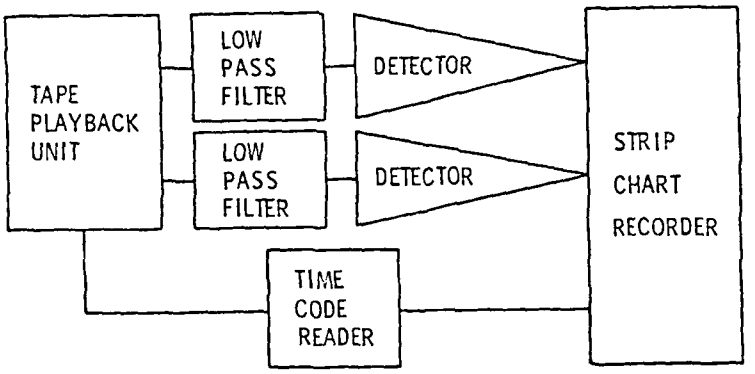

Figure 3. Block diagram of the strip charting process.

be digitized was specified. Figure 4 is a block diagram of the final digitizing system. The analog tape was played back on the Honeywell tape recorder/playback unit (Model 9600) in reverse and at a speed reduction of 4 to 1 as in the original system. With the new system, however, two channels could be digitized simultaneously. Each channel was again passed through a Spectrum, Inc. low-pass filter (Model LH-42D) set at 6 kHz with a roll-off of 24 dB per octave. The filtered data was then inputted to channels 1 and 2 of the A/D converter (Datel Model DAS-16 with control circuitry built at the Applied Research Laboratory). The A/D converter, with an input range of plus or minus 5.00 volts and sampling at a rate of 12000 Hz per channel, was started and stopped by an operator at points specified during the strip-charting process. The digitized data was fed into a 4096 × 8 bit buffer (Pertec Model BF6X9-4906) and then recorded on a nine-track Pertec Peripheral Equipment, Inc. digital tape drive (Model T9660) at 1600 bits per inch at 75 inches per second. Each sample resulted in three bytes of information written to the tape (one-half-inch IBM Multi-System Tape). These were 10 bits of data, 4 bits of channel ID, 6 bits of run number ID, and 4 bits of synchronizing information.

2.5.3 Program REVERB. The reverberation times were determined from the digitized data by means of a FORTRAN IV computer program named REVERB.[3] The hardware consisted of a 16-bit CPU, 64-byte memory core, and two cassette drives made by Interdata, Inc. (Model 7/16), Pertec tape drive (Model T9660-6-75) with interface and formatter designed and built at the Applied Research Laboratory, and

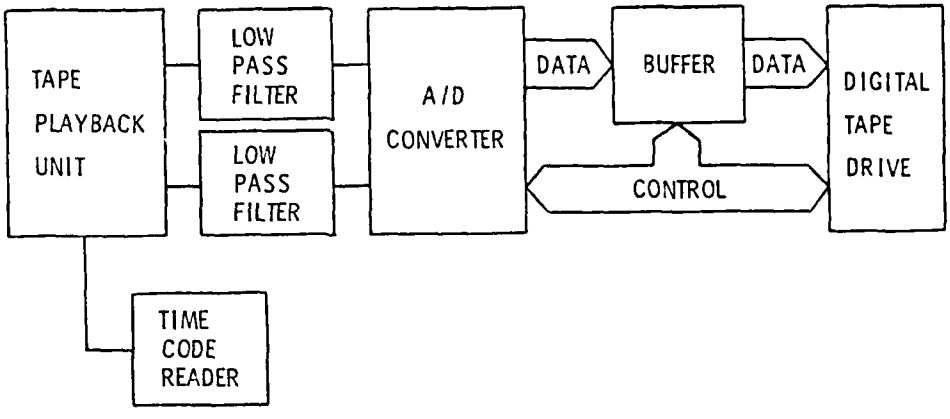

Figure 4. Block diagram of the final digitizing process.

ard copy

both made by Tektronix, Inc. REVERB's basic operations were to locate the decay, filter the data using FFT subroutines, and calculate the reverberation time using a linear, least-squares curve fit.

The menu for REVERB required that eight parameters be specified for the determination of each reverberation time. These were sample rate, ID number, file number, one-third-octave-band center frequency, search threshold, time-per-frame, back-record number, and data reel/channel number. The sample rate was set to match the sample rate at which the analog data had been digitized. The data digitized by the original digitizing system had a sample rate of 51200 samples per second; the rest of the data had a sample rate of 48000 samples per second. The ID number and file number were used to locate the required digital data for the particular decay under investigation. The one-third-octave-band center frequency controlled how the data was filtered using FFT subroutines. The search threshold was a multiplicative factor used to locate the decay itself; since the data was digitized in the reverse of real time, REVERB could determine an average value of background noise, and when data was encountered that was a specified factor greater than the background noise, then the decay had been located. For example, if search threshold were specified as 3.0, then the first data point encountered which had an amplitude of at least 3.0 times that of the average background noise could be assumed to be located somewhere on the decay. The time-per-frame parameter controlled the interval of time contained in one frame; the frame was the window of data which contained the decay,

and in terms of time economy, it was best to make the time-per-frame as short as possible considering that the reverberation times between different test conditions changed significantly. The back-record number was used to center the decay in the middle of the frame; when the search threshold value was exceeded, the FFT filtering would commence at a specified number of records back from that point. The data reel/channel number identified which test condition and hydrophone were under investigation.

In actual operation, REVERB would use the specified parameters to plot a picture of the decay on the graphic terminal. The operator, by use of a joystick, would then pick a top point and a bottom point of the decay. REVERB would then calculate a reverberation time using a linear, least-squares curve fit. The program would also subtract the level of the bottom point from the top point to give a range in dB over which the fit had been performed; ranges of less than 25 dB were generally considered too small to reasonably extrapolate to the full 60 dB required for a reverberation time. A copy of the decay, fit, reverberation time, range, and identifying parameters could then be printed on the hard copier.

CHAPTER III

RESULTS AND DISCUSSION

3.1 Reverberation Time Results

In order to determine the absorptive characteristics of the MQL tank with and without the pressure-release wall lining, REVERB was used to determine a total of 1463 reverberation times. Figure 5 is a typical result. Within this 240-millisecond window can be seen the plot of the decay in reverse, complete with background noise to the left of the decay and excitation signal to the right of the decay. Average values of the background noise and excitation signal are indicated, respectively, by the horizontal lines extending from the beginning and end of the window; these times are 50 milliseconds long, representing the time period over which these averages were performed. The beginning and end of the decay are represented by short, horizontal lines extending to the left of the points chosen by the operator. The dashed line along the decay was the slope calculated by REVERB using those top and bottom points to determine a linear, least-squares fit.

Using this technique, reverberation-time comparisons of the various test conditions and projector locations could be made. Figure 6 demonstrates that the neoprene closed-cell wall lining increased the reverberation time in the MQL tank by a factor of 3 to 4 for projector location two. Each point represents the mean value of 16 reverberation times, consisting of two data sets for each of eight hydrophones.

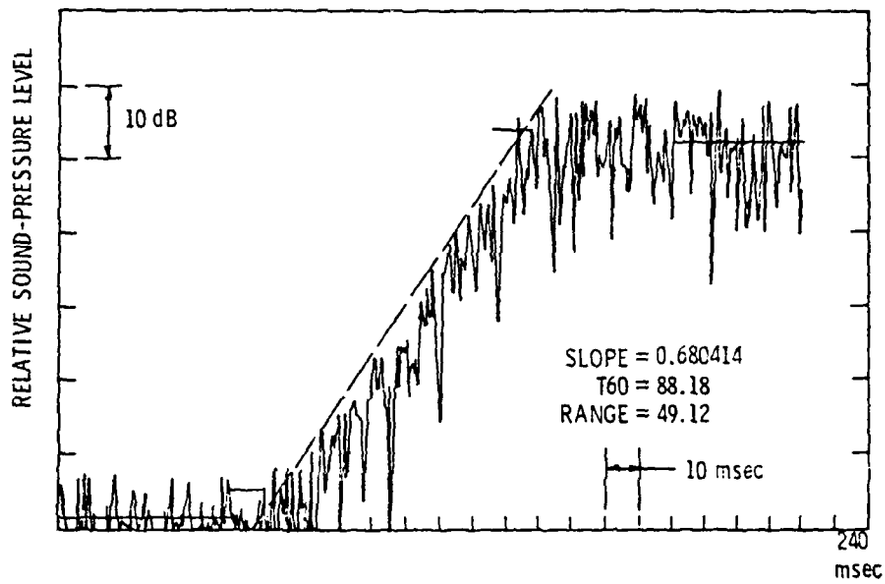

Figure 5. Plot of decay in reverse, with background noise to the left of the decay and excitation signal to the right of the decay, as produced by REVERB. Test condition IV, projector location one, hydrophone one, one-third-octave band center frequency 6.3 kHz.

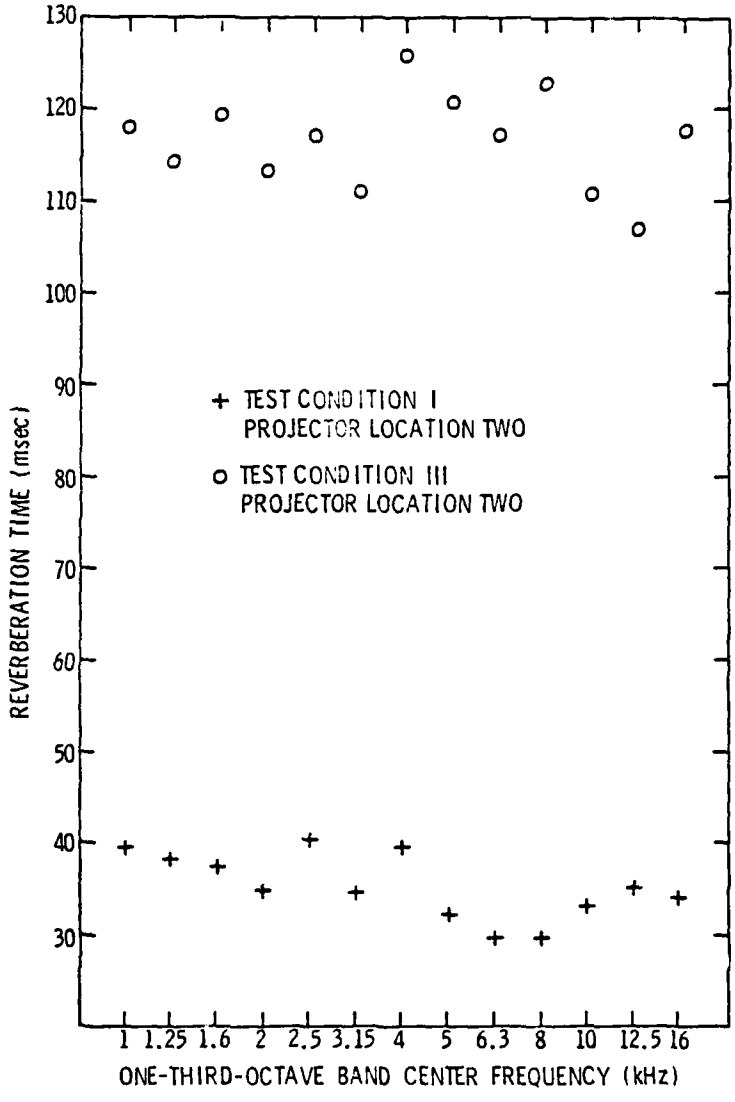

Figure 6. Graph of reverberation time as a function of one-third-octave band center frequency for test condition I. Projector location two, and test condition III, projector location two.

Each mean value is a function of one-third-octave-band center frequency, test condition, and projector location.

It became apparent during the early course of data-taking that the reverberation times were quite independent of projector location. Since the different projector locations produced similar reverberation times within each test condition and center frequency when averaged over eight hydrophone positions, the total number of 4992 data points could be drastically reduced. In order to make certain that the data was relatively independent of projector location, test condition I, which had no lining and no shell, was thoroughly investigated. For center-band frequencies 1 kHz through 1.6 kHz, three projector location data sets were completed; for center-band frequencies 2 kHz and 1o kHz through 16 kHz, four projector location data sets were completed; and for center-band frequencies 2.5 kHz through 8 kHz, five projector location data sets were completed. This represents a total of 880 reverberation times completed for test condition I. In all cases, the reverberation times were relatively independent of projector location, especially when the standard deviation was considered.

Figure 7 demonstrates the similarity in results between projector locations in test condition I. For each center-band frequency, the mean values of reverberation time for projector locations one and two are plotted next to each other along with plus and minus one standard deviation. This graph indicates that the differences between the data sets for projector locations one and two are small enough (less than 6 ms) to consider the data independent of projector

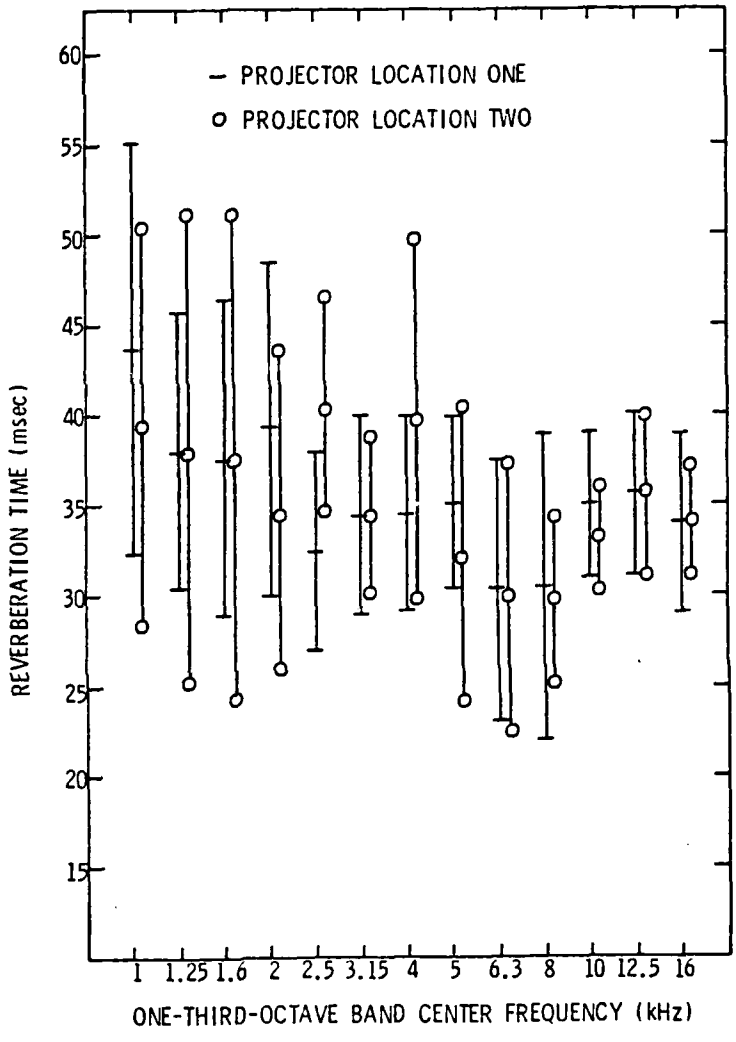

Figure 7. Graph of mean value and standard deviation of reverberation time data as a function of one-third-octave band center frequency for test condition I. Projector locations one and two.

location. It was observed that comparisons between other projector locations gave similar results for test condition I.

As a further check, two projector location data sets were completed for all thirteen center-band frequencies in test condition III, which was lined but had no shell. Again, the differences between projector location data sets were considered minor. Figure 8 demonstrates this independence for test condition III. The mean values and respective ranges of standard deviation for each center-band frequency are plotted next to each other, and the differences between projector location data sets never exceeded 10 ms. Figures 7 and 8, along with the data on Table 1, indicate that the differences between projector location data sets are small enough to consider the data independent of projector location, even in the extreme cases of lined and unlined MQL tank. Not only does this greatly reduce the required amount of data, but it allows for a much more straightforward comparison of the different test conditions; instead of having to compare test conditions as a function of projector location, test conditions can be compared directly by averaging the results of the different projector locations.

The data indicates significant differences in reverberation times between test conditions. Figure 9 and Table 2 demonstrate these differences. Test condition III, which was lined tank but no cylindrical shell, consistently had the longest reverberation times; the mean values ranged from 111.6 ms up to 123.8 ms. Test condition I, which was unlined tank but no shell, and test condition II, which was unlined tank with shell, had the shortest reverberation times.

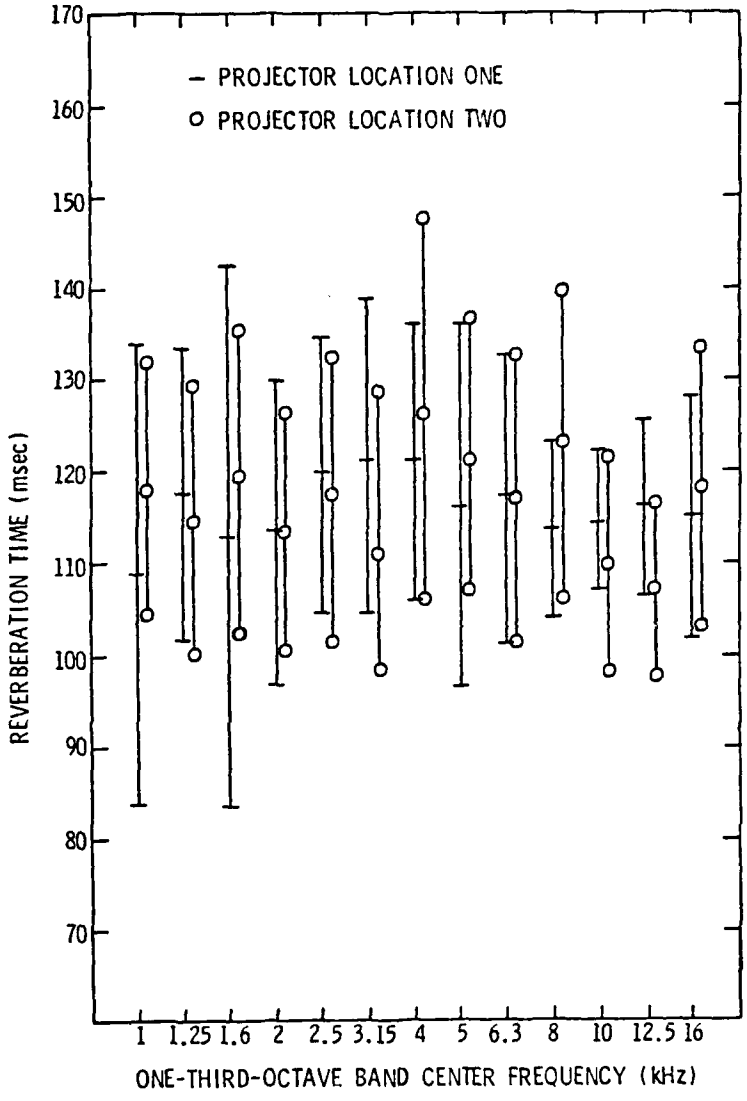

Figure 8. Graph of mean value and standard deviation of reverberation time data as a function of one-third-octave band center frequency for test condition III, projector locations one and two.

TABLE 1

REVERBERATION TIME AS A FUNCTION OF FREQUENCY AND PROJECTOR LOCATION

	Center Band Frequency (kHz)												
	1.0	1.25	1.6	2.0	2.5	3.15	4.0	5.0	6.3	8.0	10.0	12.5	16.0
TestCondition I													
Projector Location 1:													
Mean Reverberation Time, ms	43.9	38.2	37.7	39.4	32.6	34.6	34.4	35.3	30.4	30.5	35.1	35.7	34.1
Standard Deviation, ms	11.4	7.6	8.7	9.2	5.6	5.5	5.3	4.7	7.2	8.3	4.0	4.5	4.9
Projector Location 2:													
Mean Reverberation Time, ms	39.5	38.2	37.4	34.8	40.7	34.8	39.8	32.3	29.9	29.8	33.2	35.2	34.1
Standard Deviation, ms	10.9	13.0	13.6	8.8	5.9	4.4	9.9	8.2	7.3	4.5	2.8	4.6	3.1
Projector Location 3:													
Mean Reverberation Time, ms					36.0	31.2	33.9	36.0	29.7	29.3	29.9	28.9	28.9
Standard Deviation, ms					7.6	5.4	7.0	8.2	7.4	6.8	5.3	5.5	5.4
Projector Location 4:													
Mean Reverberation Time, ms	33.2	42.4	38.2	36.6	50.9	41.9	43.1	41.9	35.6	31.9	32.0	31.6	34.2
Standard Deviation, ms	11.5	8.0	6.2	6.0	10.0	6.1	11.0	8.5	5.3	6.0	4.8	8.4	5.7
Projector Location 5:													
Mean Reverberation Time, ms				39.0	37.9	39.2	37.7	32.9	33.7	33.0			
Standard Deviation, ms				8.9	4.4	7.6	7.7	4.2	3.1	4.6			
Test Condition III													
Projector Location 1:													
Mean Reverberation Time, ms	108.9	117.4	113.0	113.5	119.7	121.5	121.1	116.5	117.3	113.4	114.6	116.2	114.9
Standard Deviation, ms	24.9	15.8	29.6	16.4	15.0	17.0	15.2	19.8	15.4	9.6	7.2	9.6	13.2
Projector Location 2:													
Mean Reverberation Time, ms	118.4	114.8	119.3	113.5	117.2	111.0	126.5	121.4	117.0	123.2	110.0	107.1	114.3
Standard Deviation, ms	13.6	14.9	16.4	13.2	15.6	17.5	20.8	14.2	15.1	16.6	12.0	9.7	15.0

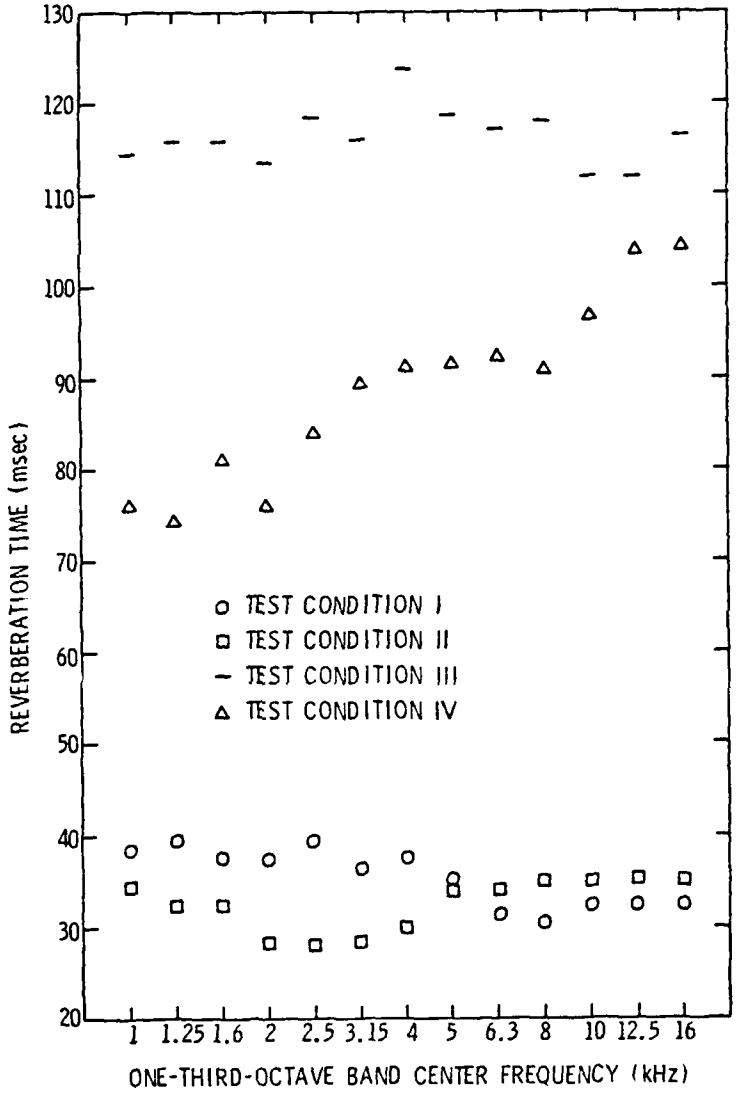

Figure 9. Graph of mean value of reverberation time data as a function of one-third-octave band center frequency for all four test conditions.

TABLE 2

REVERBERATION TIME AS A FUNCTION OF FREQUENCY AND TEST CONDITION

	Center Band Frequency (kHz)												
	1.0	1.25	1.6	2.0	2.5	3.15	4.0	5.0	6.3	8.0	10.0	12.5	16.0
Test Condition I													
Mean Reverberation Time, ms	38.9	39.6	37.8	37.6	39.6	36.5	37.5	35.5	31.6	30.6	32.5	32.8	32.8
Standard Deviation, ms	11.9	9.8	9.8	8.2	9.2	6.7	9.1	7.7	7.2	6.2	4.6	6.5	5.3
Test Condition II													
Mean Reveration Time, ms	34.8	32.3	32.2	28.7	27.4	28.4	30.2	34.1	34.0	35.0	35.3	35.8	35.2
Standard Deviation, ms	8.7	4.7	7.4	5.5	5.7	2.9	2.7	4.7	4.4	5.2	4.5	3.4	7.1
Test Condition III													
Mean Reverberation Time, ms	114.5	116.1	116.1	113.5	118.5	116.2	123.8	118.9	117.2	118.3	112.3	111.6	116.6
Standard Deviation, ms	18.8	15.2	23.8	14.7	15.1	17.8	18.1	17.1	15.0	14.2	10.0	10.6	14.0
Test Condition IV													
Mean Reverberation Time, ms	76.1	74.8	81.3	76.1	84.2	89.5	91.1	91.6	92.4	90.8	96.6	104.1	104.7
Standard Deviation, ms	19.2	12.3	21.5	15.6	15.0	20.8	12.4	15.3	10.2	11.4	10.0	9.2	4.9

Test condition II had the shortest reverberation times below 5 kHz, and test condition I had the shortest reverberation times for 6.3 kHz and higher frequencies. The mean values for test condition I ranged from 30.8 ms up to 39.6 ms; the mean values for test condition II ranged from 27.4 ms up to 35.8 ms. Test condition IV, which was lined tank with shell, lay between the other test conditions; mean values ranged from 74.8 ms up to 104.7 ms.

Figure 9 also demonstrates a very noticeable frequency dependence in test condition IV. The only difference between test conditions III and IV is the presence of the shell in test condition III. The Sabine equation

$$T_{60} = \frac{60V}{1.086\ c\Sigma S\alpha} \quad ,$$

where T_{60} is the reverberation time, V is the volume, c is the speed of sound, S is the surface area, and α is the absorption coefficient, reveals that a decrease in volume and an increase in surface area should decrease the reverberation time. The introduction of the shell into the tank displaces some of the volume and increases the surface area and also decreases the reverberation time as is to be expected. However, the general increase in reverberation time with frequency cannot be explained solely by the decrease in volume and increase in surface area. In fact, if standard deviation is considered as in Figure 10, this increase in reverberation time with frequency is great enough to cause significant overlap between test conditions III and IV in the two highest center-band frequencies.

The difference in characteristic impedance between two materials is of major importance in the relative proportion of absorption to

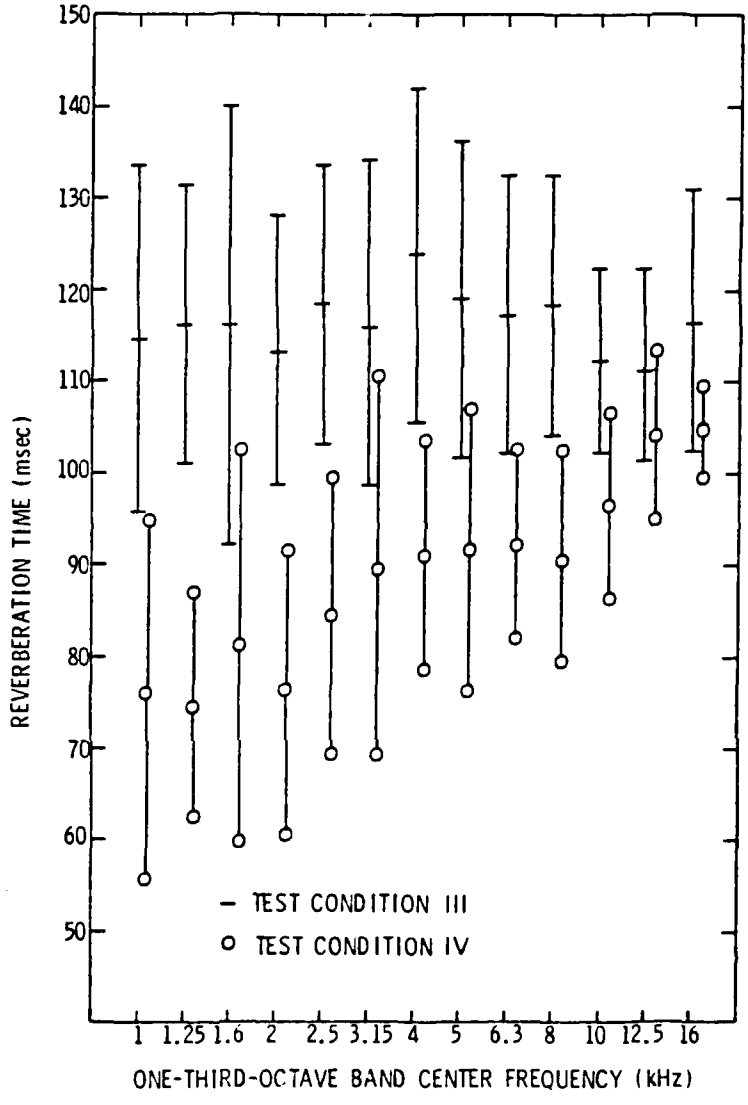

Figure 10. Graph of mean value and standard deviation of reverberation time data as a function of one-third-octave band center frequency for test conditions III and IV.

reflection of sound energy at the boundary between the two materials. In general, the greater the difference in characteristic impedance, the greater the degree of reflection and the smaller the degree of absorption; the smaller the difference in characteristic impedance, the smaller the degree of reflection and the greater the degree of absorption. The characteristic impedance of the material of the shell is an order of magnitude greater than the characteristic impedance of the surrounding water. This implies a significant amount of absorption considering that the characteristic impedance of water is approximately 3700 times greater than that of air. Although this implies that the shell is an absorber of sound energy in the tank, it still does not explain the increase of reverberation time with increasing frequency in the MQL tank with the shell present.

A comparison of test condition I to test condition II reveals this same trend. If standard deviation is taken into account, as in Figure 11, there is very significant overlap between the two test conditions. However, the presence of the shell causes the reverberation times to be slightly longer in test condition II than in test condition I for center band frequencies above 6.3 kHz. An explanation for the increase of reverberation time in the MQL tank with increasing frequency when the shell is present is that the air-filled core of the shell contributes to a decrease in characteristic impedance of the shell with increasing frequency. This decrease in characteristic impedance should make the shell more reflective with increasing frequency due to an increasing difference in characteristic impedances

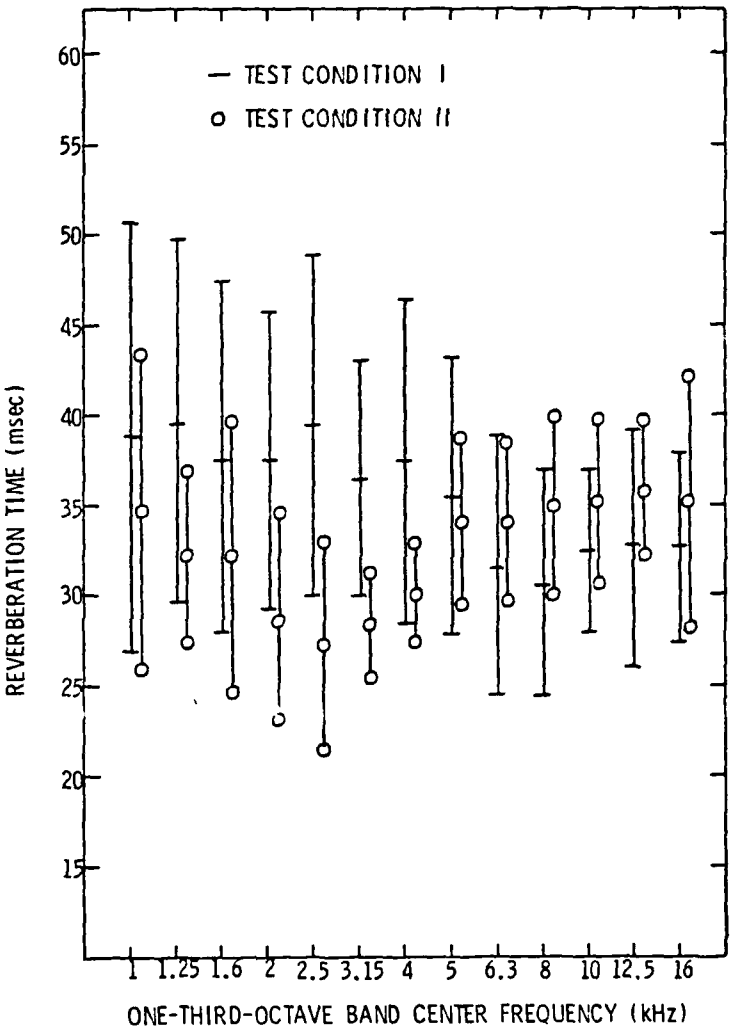

Figure 11. Graph of mean value and standard deviation of reverberation time data as a function of one-third-octave band center frequency for test conditions I and II.

between the shell and the surrounding water. As a result, as the center-band frequency increases, the shell becomes less absorptive and the reverberation time in the tank increases.

3.2 Reverberation Room Standards

The requirements for reverberation rooms in air have been established; these same requirements can also be applied to underwater reverberation chambers. However, there are several requirements which cannot be met in the MQL tank.

The requirements that no two room dimensions shall be equal nor in the ratio of small whole numbers[2] is nearly violated in the MQL tank because the width and depth are almost equal and the length is approximately three times longer than the width. The cylindrical shell which approximates equipment to be tested is much larger than the limit of 1% of the volume of the reverberation room.[1] If a piece of equipment the same size and shape as the cylindrical shell is tested as a sound source in the MQL tank, there will probably be significant contribution of the direct field to the measured mean-square pressure regardless of the position of the microphone array.[1] The minimum distance between the sound source and the nearest microphone can be calculated using the relation

$$d_{min} = 0.08 \sqrt{\frac{V}{T}} \quad ,$$

where V is the volume of the test room in cubic meters, and T is the reverberation time in seconds.[1] The water-filled volume of the MQL tank is 39.6 cubic meters, and the shortest reverberation time in test condition IV is 74.8 msec. This results in a minimum distance

of 1.8 meters; this requirement cannot be met in the MQL tank with a source of the same dimensions as the cylindrical shell. The highest value of the average absorption coefficient should not exceed 0.16;[1] this requirement necessitates that the absorption coefficients of the MQL tank be calculated from the reverberation times.

3.3 The Reverberation Equations

Problems exist with calculating absorption coefficients from reverberation times because the sound fields in rooms are extremely complex, and some simplifying assumptions must be made in order to derive useable equations. For this reason, there is no single equation which absolutely relates reverberation times to absorption coefficients. Two of the most often used equations are the Sabine equation, as given on page 32, and the Norris-Eyring equation,

$$T_{60} = \frac{60\ V}{-\ 1.086\ cS\ \ell n(1 - \bar{\alpha})} \quad ,$$

where T_{60} is the reverberation time, V is the volume, c is the speed of sound, S is the surface area, and $\bar{\alpha}$ is the average statistical absorption coefficient.

Both equations oversimplify in that they assume that the sound field is always diffuse even after the sound source has been shut off, and neglect such important factors as normal modes of vibration of the room, interference and diffraction, specific locations of various absorptive materials, and the shape of the room. There are also some important differences between the equations which can lead to unequal results. In the Sabine equation, the absorption of each surface enters individually into the denominator, whereas the Norris-Eyring equation

supposes an average statistical absorption coefficient for the whole room. The Sabine equation will not result in a vanishing reverberation time with total absorption as would be expected; however, the Norris-Eyring equation will. The Sabine equation assumes a steady, continuous absorption with time, but the Norris-Eyring equation is derived from discrete energy losses at each individual reflection. The results from both equations should be viewed with some caution, especially with higher absorption coefficients, but the Sabine equation has been recommended by Embleton[1] for use in engineering design because, for most engineering problems, published absorption coefficients used in the Sabine equation result in adequately accurate reverberation times.

3.4 Absorption Coefficients

The reverberation equations display an inverse relationship between reverberation times and absorption coefficients. Figures 12 and 13 and Tables 3 and 4 demonstrate this. Figure 12 is a graph of average absorption coefficients calculated from the mean reverberation times for the four test conditions using the Sabine equation, and Figure 13 is a graph of average absorption coefficients calculated using the Norris-Eyring equation. As would be expected from both equations, the absorption coefficients for test condition III are consistently the smallest because test condition III had the longest reverberation times. The absorption coefficients for test condition IV are larger, but generally decrease with increasing frequency. Test conditions I and II have the largest absorption coefficients; test condition II has the largest absorption coefficients for 5 kHz and below, while test condition I has the largest absorption coefficients for 6.3 kHz and up.

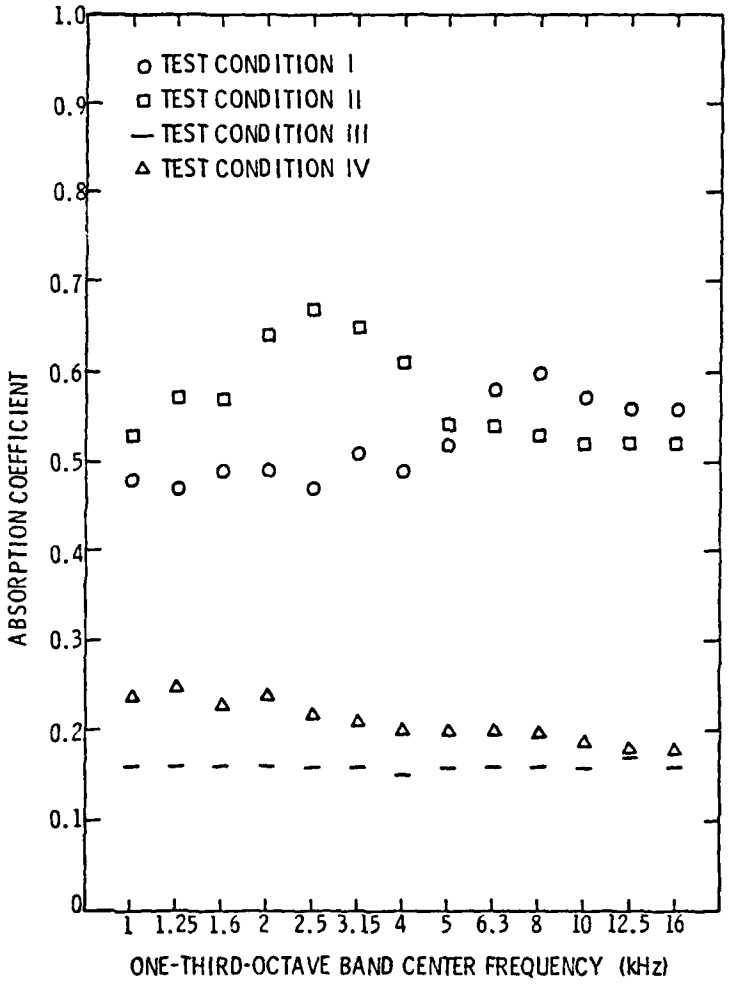

Figure 12. Absorption coefficients calculated from the Sabine reverberation equation using mean values of reverberation time as a function of one-third-octave band center frequency.

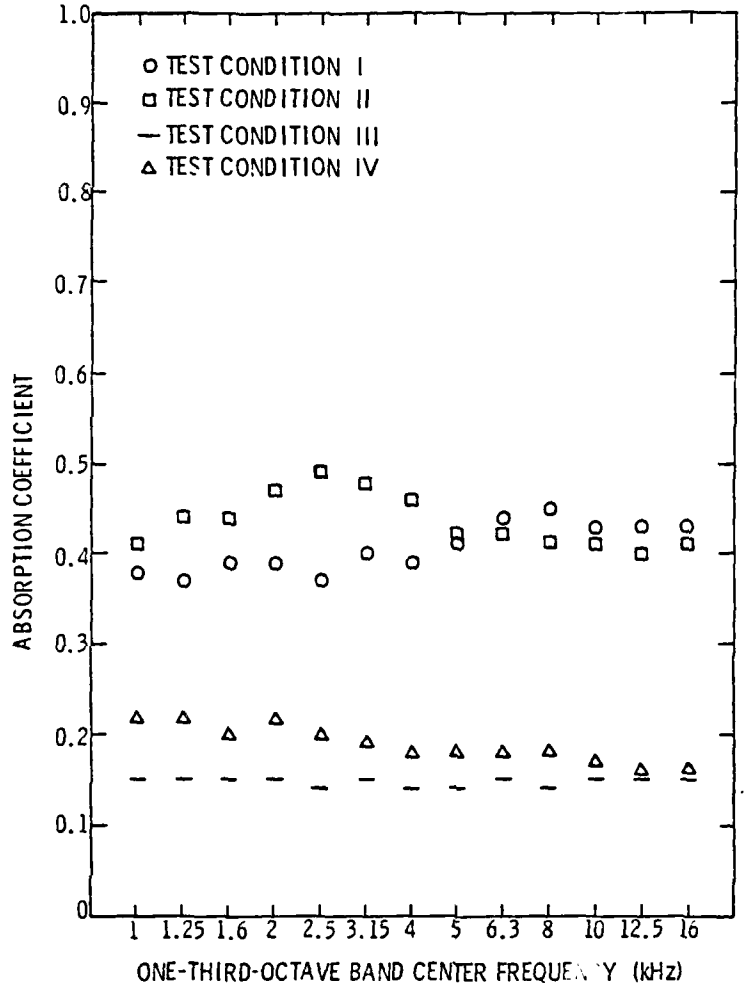

Figure 13. Absorption coefficients calculated from the Norris-Eyring reverberation equation using mean values of reverberation time as a function of one-third-octave band center frequency.

TABLE 3

ABSORPTION COEFFICIENTS CALCULATED FROM THE SABINE EQUATION

	Center Band Frequency (kHz)												
	1.0	1.25	1.6	2.0	2.5	3.15	4.0	5.0	6.3	8.0	10.0	12.5	16.0
Test Condition I:													
Absorption Coefficient	0.48	0.47	0.49	0.49	0.47	0.51	0.49	0.52	0.58	0.60	0.57	0.56	0.56
Minimum Absorption Coefficient	0.36	0.37	0.39	0.40	0.38	0.43	0.40	0.43	0.48	0.50	0.50	0.47	0.48
Maximum Absorption Coefficient	0.69	0.62	0.66	0.63	0.61	0.62	0.65	0.66	0.75	0.75	0.66	0.70	0.67
Test Condition II:													
Absorption Coefficient	0.53	0.57	0.57	0.64	0.67	0.65	0.61	0.54	0.54	0.53	0.52	0.52	0.52
Minimum Absorption Coefficient	0.42	0.50	0.47	0.54	0.56	0.59	0.56	0.48	0.48	0.46	0.46	0.47	0.44
Maximum Absorption Coefficient	0.71	0.67	0.74	0.80	0.85	0.72	0.67	0.63	0.62	0.62	0.60	0.57	0.65
Test Condition III:													
Absorption Coefficient	0.16	0.16	0.16	0.16	0.16	0.16	0.15	0.16	0.16	0.16	0.16	0.17	0.16
Minimum Absorption Coefficient	0.14	0.14	0.13	0.14	0.14	0.14	0.13	0.14	0.14	0.14	0.15	0.15	0.14
Maximum Absorption Coefficient	0.19	0.18	0.20	0.19	0.18	0.19	0.17	0.18	0.18	0.18	0.18	0.18	0.18
Test Condition IV:													
Absorption Coefficient	0.24	0.25	0.23	0.24	0.22	0.21	0.20	0.20	0.20	0.20	0.19	0.18	0.18
Minimum Absorption Coefficient	0.19	0.21	0.18	0.20	0.19	0.17	0.18	0.17	0.18	0.18	0.17	0.16	0.17
Maximum Absorption Coefficient	0.32	0.30	0.31	0.31	0.27	0.27	0.23	0.24	0.22	0.23	0.21	0.19	0.18

TABLE 4

ABSORPTION COEFFICIENTS CALCULATED FROM THE NORRIS-EYRING EQUATION

	Center Band Frequency (kHz)												
	1.0	1.25	1.6	2.0	2.5	3.15	4.0	5.0	6.3	8.0	10.0	12.5	16.0
Test Condition I:													
Absorption Coefficient	0.38	0.37	0.39	0.39	0.37	0.40	0.39	0.41	0.44	0.45	0.43	0.43	0.43
Minimum Absorption Coefficient	0.31	0.31	0.32	0.33	0.31	0.35	0.33	0.35	0.38	0.39	0.39	0.37	0.38
Maximum Absorption Coefficient	0.50	0.46	0.48	0.47	0.46	0.46	0.48	0.49	0.53	0.53	0.48	0.50	0.49
Test Condition II:													
Absorption Coefficient	0.41	0.44	0.44	0.47	0.49	0.48	0.46	0.42	0.42	0.41	0.41	0.40	0.41
Minimum Absorption Coefficient	0.35	0.39	0.37	0.42	0.43	0.45	0.43	0.38	0.38	0.37	0.37	0.38	0.35
Maximum Absorption Coefficient	0.51	0.49	0.53	0.55	0.57	0.51	0.49	0.47	0.46	0.46	0.45	0.43	0.48
Test Condition III:													
Absorption Coefficient	0.15	0.15	0.15	0.15	0.14	0.15	0.14	0.14	0.15	0.14	0.15	0.15	0.15
Minimum Absorption Coefficient	0.13	0.13	0.12	0.13	0.13	0.13	0.12	0.13	0.13	0.13	0.14	0.14	0.13
Maximum Absorption Coefficient	0.18	1.17	0.18	0.17	0.16	0.17	0.16	0.17	0.17	0.16	0.17	0.17	0.16
Test Condition IV:													
Absorption Coefficient	0.22	0.22	0.20	0.22	0.20	0.19	0.18	0.18	0.18	0.18	0.17	0.16	0.16
Minimum Absorption Coefficient	0.18	0.19	0.16	0.18	0.17	0.15	0.16	0.16	0.16	0.17	0.16	0.15	0.15
Maximum Absorption Coefficient	0.28	0.26	0.27	0.26	0.23	0.24	0.21	0.21	0.20	0.21	0.19	0.18	0.17

Test conditions I and II had no pressure-release wall lining. Figure 14 shows that regardless of which of the two equations are used, the absorption coefficients for test conditions I and II are too high to consider the unlined MQL tank for use as a reverberation chamber. The Sabine absorption coefficients for test condition I range from 0.47 to 0.60; the Norris-Eyring absorption coefficients for test condition I follow the same general contour but are lower, ranging from 0.37 to 0.45. The Sabine absorption coefficients for test condition II range from 0.52 to 0.67; the Norris-Eyring absorption coefficients again follow the same general contour and are lower, ranging from 0.40 to 0.49.

Test conditions III and IV had the pressure-release wall lining. Figure 15 shows that the pressure-release wall lining reduced the absorption coefficients enough to consider the MQL tank as a candidate for a reverberation chamber, especially in test condition III. The Sabine absorption coefficients for test condition III are all 0.16 except for one value of 0.15 at 4 kHz and 0.17 at 12.5 kHz; for test condition IV, the Sabine absorption coefficients range from 0.18 to 0.25. The Norris-Eyring absorption coefficients for test condition III are all 0.15 except for four values of 0.14; for test condition IV, the Norris-Eyring absorption coefficients range from 0.16 to 0.22.

The absorption coefficients produced by the two equations are in much better agreement for lower values as in test conditions III and IV than for the higher values in test conditions I and II. This can be seen in Figures 16 and 17 and Tables 3 and 4 in which minimum and maximum absorption coefficients are included as a range for each absorption coefficient. The minimum absorption coefficient is found

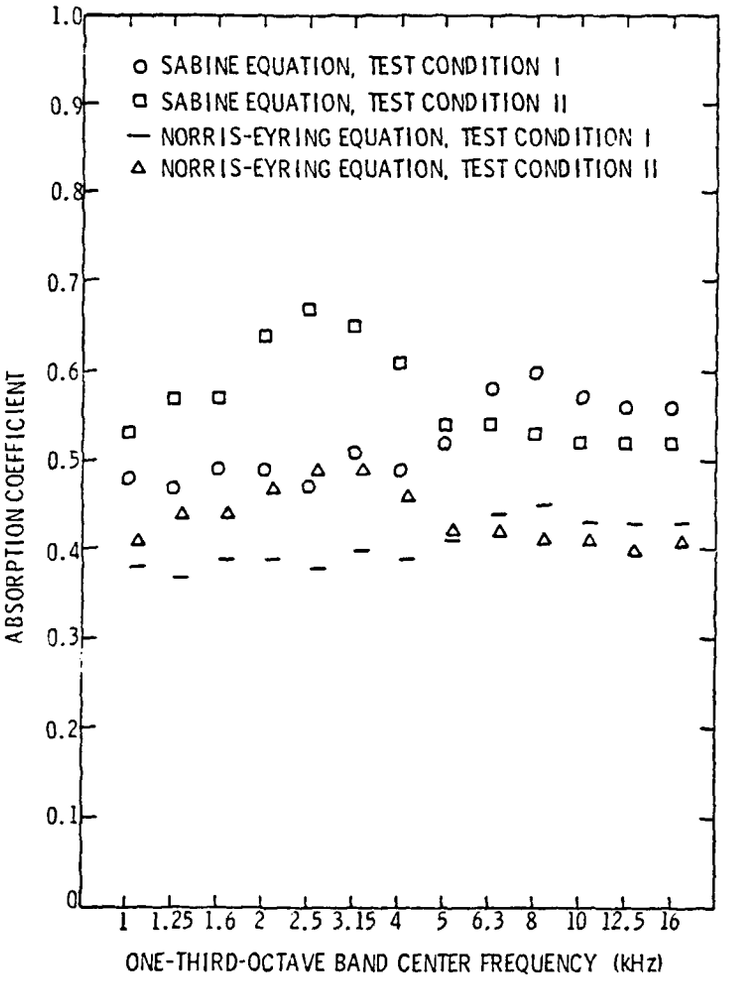

Figure 14. Graphical comparison of absorption coefficients as calculated from the Sabine and Norris-Eyring equations for test conditions I and II.

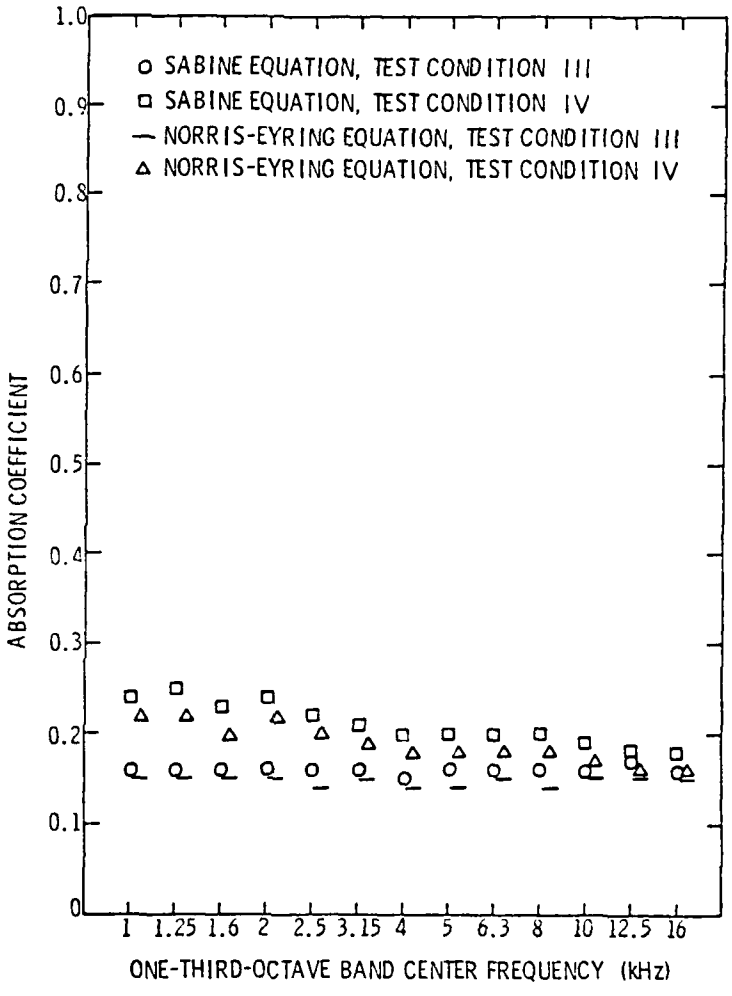

Figure 15. Graphical comparison of absorption coefficients as calculated from the Sabine and Norris-Eyring equations for test conditions III and IV.

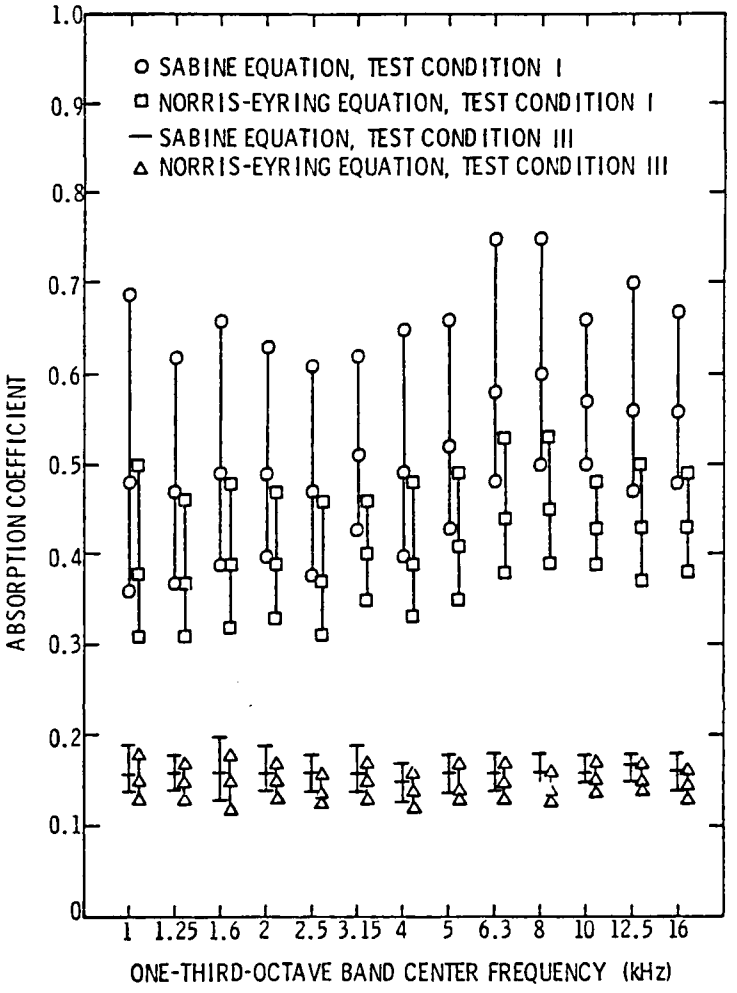

Figure 16. Minimum, mean, and maximum absorption coefficients as calculated from the Sabine and Norris-Eyring equations for test conditions I and III.

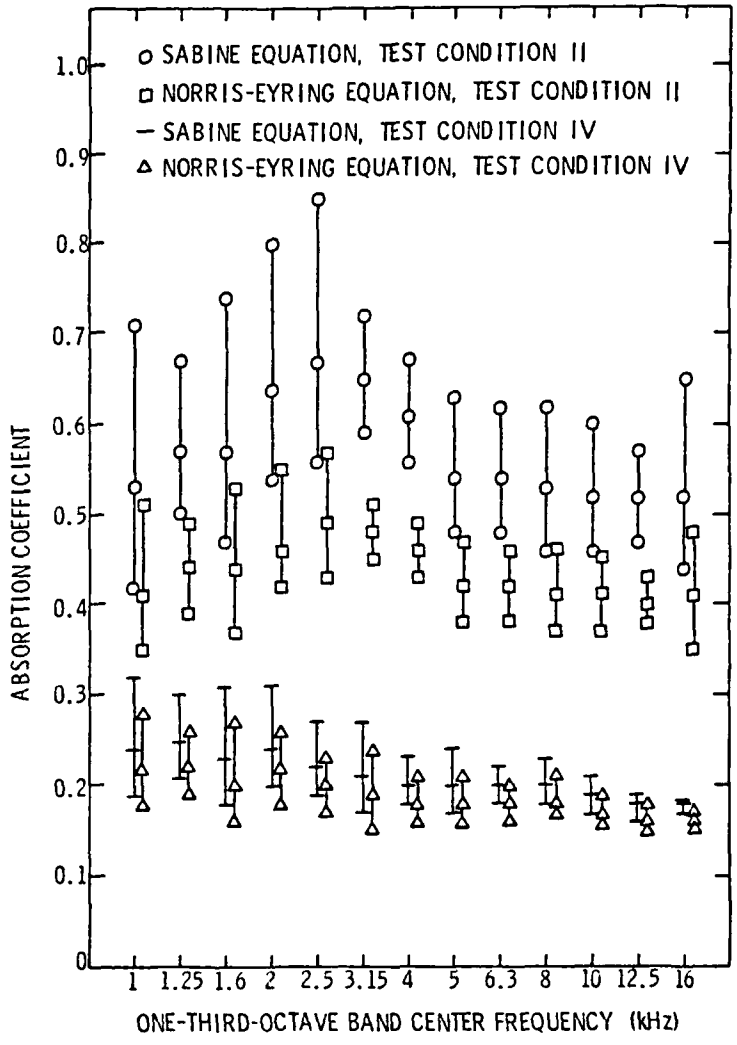

Figure 17. Minimum, mean, and maximum absorption coefficients as calculated from the Sabine and Norris-Eyring equations for test conditions II and IV.

by adding the standard deviation of reverberation time to the mean reverberation time, and using the result in each of the reverberation equations. The maximum absorption coefficient is found in the same manner except that the standard deviation is subtracted instead of added to the mean reverberation time. The minimum and maximum absorption coefficients highlight the very good agreement between the Sabine and Norris-Eyring equations for the low values of absorption coefficients in test conditions III and IV, and the lack of agreement for higher values on test conditions III and IV.

3.5 Theoretical Check

In order to check the accuracy of the reverberation times obtained through the use of a digital computer and the absorption coefficients calculated from the reverberation times, absorption coefficients were calculated theoretically. This was done by calculating the reflection coefficient at the boundary between two mediums with different characteristic impedances, using the reflection coefficient to derive an absorption coefficient for each boundary, then summing the products of absorption coefficient and the appropriate surface area to get an average absorption coefficient for the MQL tank.

Using the equation

$$c_r = \frac{\rho_2 c_2 \cos\theta_i - \rho_1 c_1}{\rho_2 c_2 \cos\theta_i + \rho_1 c_1} \quad ,$$

where c_r is the reflection coefficient, $\rho_1 c_1$ is the characteristic impedance of the water which is 1.48×10^6 MKS rayls, $\rho_2 c_2$ is the characteristic impedance of the air which is 415 MKS rayls or the

concrete which is 8.0×10^6 MKS rayls,[15] and θ_i is the angle at which the sound is incident on the air or concrete, the reflection coefficient was calculated for the two cases of the water/air boundary and the water/concrete boundary. It should be noted that this equation assumes a locally-reacting medium, and that this equation is angle-dependent and frequency-independent.

Since the angles of incidence in the MQL tank were somewhat random, the reflection coefficient was calculated for every 5° from 0° to 90° for both water/air and water/concrete boundaries. Each of these reflection coefficients was used in the equation

$$\alpha = 1 - |c_r|^2 \quad ,$$

where α is the absorption coefficient, to find an absorption coefficient corresponding to each reflection coefficient. These absorption coefficients were then added together and divided by the number of angles to derive a frequency-independent coefficient for each of the water/air and water/concrete boundaries. In this manner, the water/air absorption coefficient α_{WA} was calculated to be 0.00070, and the water/concrete absorption coefficient α_{WC} was calculated to be 0.66.

These absorption coefficients were then multiplied by the appropriate surface areas. The top surface, which was a water/air boundary for all test conditions, had a surface area of 18.6 square meters. Multiplying this surface area by α_{WA} resulted in 0.013 m^2. The bottom surface, which was a water/concrete boundary for all test conditions, also had a surface area of 18.6 square meters. Multiplying

this surface area by α_{WC} resulted in 12.3 m^2. The walls had a total surface area of 42.8 square meters. For test conditions I and II, the walls were a water/concrete boundary. Multiplying this surface area by α_{WC} resulted in 28.2 m^2. Summing these products of surface areas and appropriate absorption coefficients resulted in a total of 40.5 m^2. When this value was divided by the total surface area, 80.1 m^2, the theoretical average absorption coefficient for the MQL tank for test conditions I and II was found to be 0.51. For test conditions III and IV, the wall lining was in place. Since the wall lining was made of closed-cell neoprene, which is mostly air and acted as a pressure-release boundary, the wall lining was considered a water/air boundary. Multiplying this surface area by α_{WA} resulted in 0.030 m^2. Summing these products of surface areas and appropriate absorption coefficients resulted in a total of 12.3. When this value was divided by the total surface area, the theoretical average absorption coefficient for the MQL tank for test conditions III and IV was found to be 0.15.

The theoretical average absorption coefficients agree quite well with the absorption coefficients calculated from the reverberation times. Figure 18 shows that the theoretical value of 0.51 for the MQL tank with no wall lining runs through the center of the range of absorption coefficients for test conditions I and II which had no wall lining. Figure 19 shows that the theoretical value of 0.15 for the MQL tank with wall lining agrees well with the absorption coefficients for test conditions III and IV which had the wall lining, and especially well for test condition III.

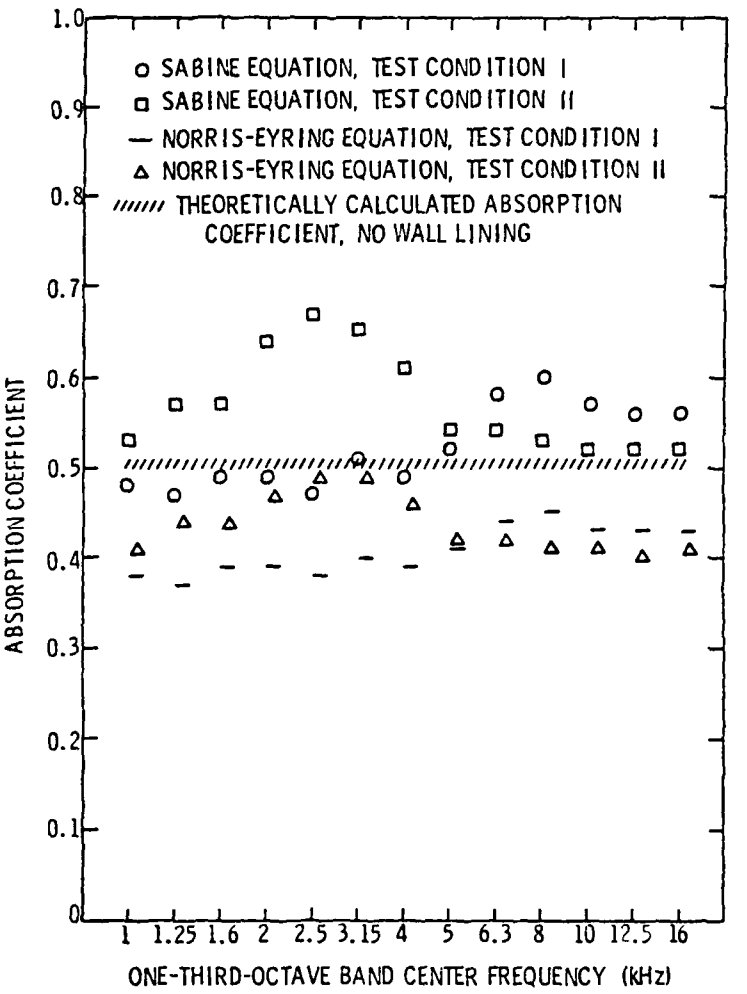

Figure 18. Sabine and Norris-Eyring absorption coefficients for test conditions I and II, and the theoretically calculated absorption coefficient for the MQL tank with no wall lining.

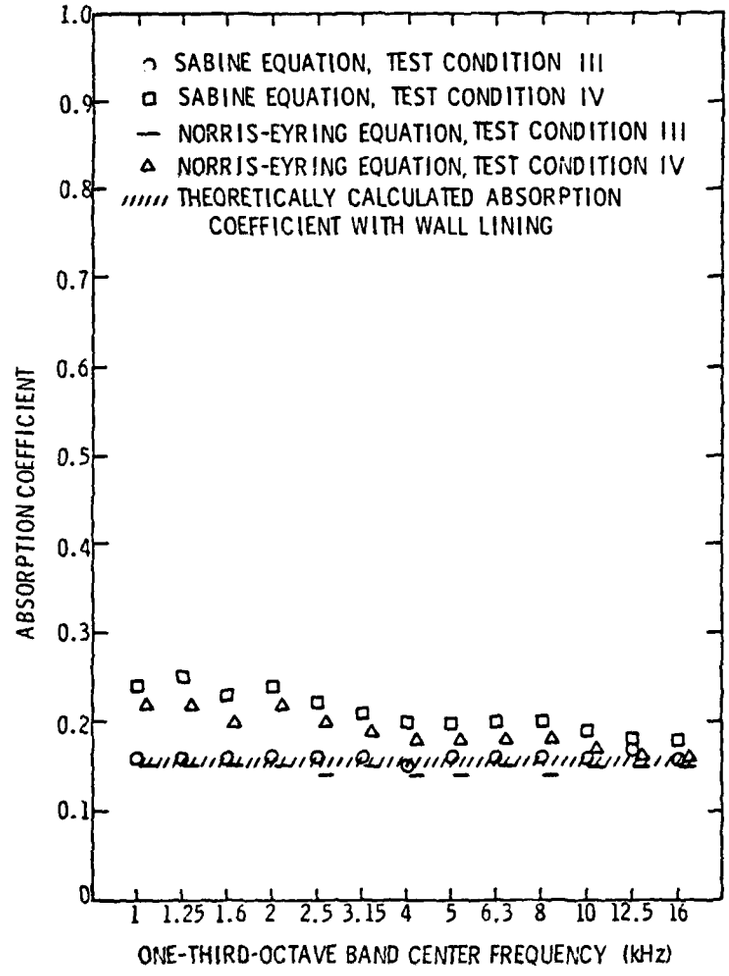

Figure 19. Sabine and Norris-Eyring absorption coefficients for test conditions III and IV, and the theoretically calculated absorption coefficient for the MQL tank with wall lining.

It should be noted that this method of calculating theoretical absorption coefficients is a very rough approximation. The process of calculating the values of reflection coefficient for every 5° gives an unduly equal weighting to each of these values of incidence. This can be very misleading, because the angle of incidence of a sound wave makes a significant difference in the amount of energy absorbed. For example, a sound wave normally incident on an absorbing boundary will have much more energy absorbed than a sound wave with grazing incidence. A more accurate absorption coefficient can be calculated from the "Paris' formula",[6]

$$\alpha = 2\int_{o}^{\pi/2} \alpha(\theta)\, \cos\theta \sin\theta d\theta \quad ,$$

where $\alpha(\theta)$ is the angle-dependent absorption coefficient as can be derived from the equations given on pages 48 and 49.

CHAPTER IV

CONCLUSIONS AND RECOMMENDATIONS

The absorption coefficients for test conditions I and II are all too large for use in a reverberant chamber. The wall lining drastically reduces the absorption coefficients to the point that test conditions III and IV could be considered suitable for a reverberant chamber. Test condition III in particular meets all of the requirements for a reverberant chamber.

It is possible to calculate the sound power of a sound source in a reverberant chamber by using an equation suggested by Blake and Maga.[7] This equation relates the output power of the source π_S to the mean-square pressure of the resultant reverberant sound field $\langle p \rangle^2$ by

$$\pi_S = \frac{13.8\ V}{\rho_o c_o^2\ T_{60}\ (1 - \alpha)} \langle p \rangle^2 \quad ,$$

where V is the volume in m^3, ρ_o is the density of water in kg/m^3, c_o is the speed of sound in water in m/sec, T_{60} is the reverberation time in sec, and α is the appropriate absorption coefficient.

The introduction of the cylindrical shell as in test condition IV presents some problems. It raises the average absorption coefficients, especially toward the lower frequencies, such that caution is necessary if the MQL tank is to be used as a reverberant chamber. Furthermore, if a sound source with the same size, shape,

and orientation as the cylindrical shell is used in the MQL tank. It would be difficult to insure that any hydrophone position would be out of the direct field and in the reverberant field. Some preliminary investigation into the directivity patterns, absorptive characteristics, and resonant characteristics of such a source would prove helpful for the best possible use of the MQL tank. Furthermore, an investigation of reverberation times with frequencies higher than 16 kHz could show that the MQL tank could be used as an underwater reverberation chamber with relatively large sound sources at higher frequencies. On the other hand, it seems reasonable to assume that sound sources which are smaller than 1% of the total volume could be conveniently and correctly used in the MQL tank.

A study of the sound field in the MQL tank on a statistical basis is recommended for a more detailed description of the modal density and modal overlap, and to determine a lower limit on the frequencies for which the MQL tank can be used with reliability. Furthermore, other methods of determining reverberation times should be implemented in order to verify the results of this digital analysis method and to compare the relative ease and accuracy of determining reverberation times with different methods.

REFERENCES

1. ANS S1.21-1972, Methods for the Determination of Sound Power Levels of Small Sources in Reverberation Rooms, American National Standards Institute, New York, NY.

2. ANS S1.7-1970 (ASTM C 423-66)(R1972), Standard Method of Test for Sound Absorption of Acoustical Materials in Reverberation Rooms, American National Standards Institue, New York, NY.

3. Fridrich, R. J. "Reverberation Time Measurements in an Underwater Chamber With and Without a Pressure-Release Wall Covering," MS Thesis, Acoustics, November 1978, The Pennsylvania State University, University Park, PA.

4. Beranek, L. L. Noise and Vibration Control, New York, NY: McGraw-Hill, 1971.

5. Kinsler, L. E., and Frey, A. R. Fundamentals of Acoustics, New York, NY: John Wiley and Sons, Inc., 1962.

6. Kuttruff, H. Room Acoustics, New York, NY: John Wiley and Sons, Inc., 1973.

7. Blake, W. K., and Maga, L. J. "Chamber for Reverberant Acoustic Power Measurements in Air and in Water," J. Acoust. Soc. Am., 57, 380 (1975).

DISTRIBUTION LIST FOR TM 81-150

Commander (NSEA 0342)
Naval Sea Systems Command
Department of the Navy
Washington, DC 20362 — Copies 1 and 2

Commander (NSEA 9961)
Naval Sea Systems Command
Department of the Navy
Washington, DC 20362 — Copies 3 and 4

Defense Technical Information Center
5010 Duke Street
Cameron Station
Alexandria, VA 22314 — Copies 5 through 10


DAT
FILM